Electronic Supplementary Material (ESI) for Chemical Communications
This journal is © The Royal Society of Chemistry 2011

Insulated Copper(I) "Wires": Structural Variations and Photoluminescence

Oleksandr Hietsoi, Cristina Dubceac, Alexander S. Filatov and Marina A. Petrukhina*

Department of Chemistry, University at Albany, State University of New York,

1400 Washington Avenue, Albany, New York 12222, USA

SUPPLEMENTARY INFORMATION

Experimental details

General procedures

All synthetic reactions and manipulations were carried out under a dry dinitrogen atmosphere using standard Schlenk and vacuum-line techniques. Sublimation-deposition procedures were performed in small glass ampoules (*ca.* 7 cm long with an O.D. of 1.1 cm), which were sealed under reduced pressure (*ca*. 10−2 Torr) and then placed in electric furnaces having a small temperature gradient along the length of the tube.

Starting materials

Benzene and hexanes were dried over sodium/benzophenone under argon and were freshly distilled prior to use. 1,2-dichlorobenzene, anhydrous, 99%, was obtained from Sigma-Aldrich, degassed and dried over molecular sieves prior to use. 2,4,6-triisopropylbenzoic acid was purchased from Alfa Aesar, 97%; copper(I) acetate, 90%, was purchased from Acros and used as received.

Physical measurements. The IR spectra were recorded on a Perkin Elmer FT-IR Spectrometer (Spectrum 100) in the 4000–600 cm^{-1} range, using a universal ATR accessory. The room temperature photoluminescence (PL) spectra of crystalline powders were collected on a HORIBA Jobin Yvon spectrofluorimeter using front-face detection. Three full scans were recorded in each case and then averaged. Default hardware settings (the slit width of 5 nm and integration time of 0.1 s) were applied. Thermogravimetric measurements were carried out under nitrogen using a TGA 2050 Thermogravimetric Analyzer, TA Instruments, Inc. Elemental analyses were performed by Complete Analysis Laboratories, Inc., New Jersey, US.

Synthetic procedures

Synthesis of $[Cu(O_2C_{16}H_{23})]_\infty$ (1): A mixture of 0.10 g of copper(I) acetate (0.41 mmol), 0.50 g of 2,4,6-triisopropylbenzoic acid (2.02 mmol) (1:2.5) and 0.05 g of metallic copper in 40 mL of *m*-xylene was refluxed for 43 h with a Dean-Stark trap. The obtained light brown solution was filtered through Celite and then concentrated to dryness affording a brown solid. This solid was washed 4 times with hexanes (4 x 10 mL) until it was completely off-white. The powder was dried under vacuum in a sand bath at 65 °C for 12 h. Yield: 0.25 g, 99%. Anal. Calc. for $C_{16}H_{23}CuO_2$: C, 61.81; H, 7.46. Found: C, 61.72; H, 7.35%. PL (λ_{ex} = 350 nm, λ_{max}, nm) 535. IR (ν_{max}/cm^{-1}): 2957m, 2925w, 2869w, 1609w, 1577w, 1518s, 1476m, 1460m, 1404s, 1382w, 1361w, 1342w, 1320w, 1300w, 1244w, 1157w, 1108w, 1072w, 941w, 873m, 857w, 813w, 781w. The experimental X-ray powder pattern is different from the calculated powder patterns based on the single crystal unit cell parameters for **2** or **3** (Fig. S7).

Synthesis of $[Cu(O_2C_{16}H_{23})]_{\infty,linear}$ (2): Colorless long thin needles of **2** suitable for the single crystal X-ray diffraction analysis were obtained by sublimation of **1** at 186 °C over 2 months. Yield: 0.028g, 93%. The 70% yield can be achieved over 5 days. PL (λ_{ex} = 350 nm, λ_{max}, nm) 563. IR (ν_{max}/cm^{-1}): 2956m, 2928w, 2866w, 1606w, 1576w, 1512s, 1482m, 1463m, 1421s, 1380w, 1361m, 1319w, 1240w, 1171w, 1158w, 1109w, 1071w, 1055w, 951w, 940w, 923w, 875m, 859w, 814w, 799w, 769m. The experimental X-ray powder pattern of the bulk material is consistent with the calculated powder pattern based on the single crystal unit cell parameters for **2** (Fig. S5).

Synthesis of $[Cu(O_2C_{16}H_{23})]_{\infty,zigzag}$ (3). Colorless blocks of **3** suitable for the single crystal X-ray diffraction analysis were obtained by sublimation of **1** at 214 °C in 4 days. Crystals of **3** appear as a mixture with **2** but can be easily separated. Yield: 0.016g, 53%. PL (λ_{ex} = 350

nm, λ_{max}, nm) 610. IR (ν_{max}/cm^{-1}): 2958m, 2926w, 2866w, 1606w, 1574w, 1543s, 1520s, 1478w, 1456m, 1417s, 1379m, 1362w, 1354w, 1319w, 1240w, 1158w, 1109w, 1067w, 1055w, 941w, 878m, 859w, 815w, 765m. The experimental X-ray powder pattern of the bulk material is consistent with the calculated powder pattern based on the single crystal unit cell parameters for **3** (Fig. S6).

Synthesis of [$Cu_2(O_2C_{16}H_{23})_2 \cdot 2C_6H_4Cl_2$] (4). 0.05 g of **1** was dissolved upon heating in 2 mL of 1,2-dichlorobenzene forming a light-yellow solution. The hot solution was filtered by cannula into a 50 mL Schlenk tube and kept at 12 °C for 12 h. Colorless blocks of **4** were collected from the bottom of the tube. Yield: 0.03 g, 41%. Anal. Calc. for $C_{44}H_{54}Cu_2Cl_4O_4$: C, 57.71; H, 5.94. Found: C, 57.67; H, 6.03%. PL (λ_{ex} = 350 nm) no detectable emmision. IR (ν_{max}/cm^{-1}): 2955w, 2925w, 2866w, 1607w, 1574w, 1525s, 1483w, 1453m, 1434w, 1416s, 1380w, 1360w, 1343w, 1318w, 1249w, 1156w, 1124w, 1112w, 1070w, 1029m, 944w, 880w, 857w, 810w, 790w, 781w, 753s, 736w. The experimental X-ray powder pattern of the crystalline bulk material is consistent with the calculated powder pattern based on the single crystal unit cell parameters for **4** (Fig. S8).

Transformation of 2 to 3. Crystals of **2** can be sublimed at 214 °C to form **3**. See procedure above for the synthesis of **3** from the bulk material.

Transformation of 2 and 3 to 1. Recrystallization of **2** or **3** from benzene, toluene, or *m*-xylene (or from hexanes using solvothermal conditions) provides **1** that, in turn, can be converted to either **2** or **3** using gas-phase sublimation procedures.

X-ray crystallographic procedures

The X-ray intensity data were collected for **2–4** on a Bruker APEX CCD X-ray diffractometer equipped with a graphite monochromated Mo Kα radiation source (λ = 0.71073 Å). Data reduction and integration were performed with the software package *SAINT*,[1] and absorption corrections were applied using the program *SADABS*.[2] All structures were solved and refined using the *SHELXTL* program package.[3] All non-hydrogen atoms were refined anisotropically. Hydrogen atoms were included at idealized positions as a riding model. In **2**, two isopropyl groups were found disordered. Each disorder was individually modeled over two orientations with a 1:1 ratio. The disordered parts were restrained to be similar (SAME command in SHELXL). Three atoms from the disordered groups (C8X, C11Y, C13X) were restrained to be approximately isotropic with the ISOR command. Crystallographic data and X-ray experimental conditions for **2**−**4** and 2,4,6-triisopropylbenzoic acid are listed in Table S1. Selected bond distances (Å) and angles (º) for $[Cu(O_2C_{16}H_{23})]_\infty$ (**2**), $[Cu(O_2C_{16}H_{23})]_\infty$ (**3**), $[Cu_2(O_2C_{16}H_{23})_2]\cdot 2\ C_6H_4Cl_2$ (**4**), $[Cu(O_2C(3,5\text{-}CF_3)_2C_6H_3)]_\infty$ and $[Cu(O_2CC(CH_3)_3)]_\infty$ are collected in Table S2.

Table S1. Crystallographic data and X-ray experimental conditions for $[Cu(O_2C_{16}H_{23})]_{\infty,\ linear}$ (**2**), $[Cu(O_2C_{16}H_{23})]_{\infty,\ zigzag}$ (**3**), $[Cu_2(O_2C_{16}H_{23})_2]\cdot 2C_6H_4Cl_2$ (**4**) and $C_{16}H_{23}O_2H$.

	2	**3**	**4**	$C_{16}H_{23}O_2H$
Empirical formula	$C_{16}H_{23}CuO_2$	$C_{16}H_{23}CuO_2$	$C_{44}H_{54}Cl_4Cu_2O_4$	$C_{16}H_{24}O_2$
Formula weight	310.88	310.88	915.77	248.35
T (K)	100(2)	100(2)	100(2)	100(2)
Crystal description	needle	plate	block	needle
Crystal color	colorless	colorless	colorless	colorless
Crystal system	monoclinic	orthorhombic	monoclinic	triclinic

Space group	$P2_1/c$	$Pbcn$	$P2_1/c$	$P\bar{1}$
a (Å)	17.979(3)	34.687(3)	8.4789(9)	7.847(3)
b (Å)	5.7850(10)	10.2092(8)	11.4630(13)	9.339(3)
c (Å)	15.146(3)	8.5888(7)	22.026(2)	11.335(4)
α (º)	90.00	90.00	90.00	94.552(6)
β (º)	104.285(3)	90.00	92.125(2)	99.047(6)
γ (º)	90.00	90.00	90.00	112.924(5)
V (Å^3)	1526.5(5)	3041.5(4)	2139.3(4)	746.5(4)
Z	4	8	2	2
Reflections measured/unique	10313/2688	24294/3638	18036/4987	6540/3360
R_{int}	0.0381	0.0396	0.0371	0.0326
$R1^a$, $wR2^b$ [$I > 2\sigma(I)$]	0.0609, 0.1667	0.0375, 0.0966	0.0341, 0.0879	0.0507, 0.1348
$R1^a$, $wR2^b$ (all data)	0.0726, 0.1756	0.0425, 0.1003	0.0402, 0.0919	0.0601, 0.1436
Quality-of-fit^c	1.074	1.086	1.047	1.060
Largest diff. peak/hole, e/Å^3	1.341, -0.629	1.247, -0.367	0.894, -0.325	0.309, -0.360

$^a R1 = \Sigma\big|\,|F_o| - |F_c|\,\big| / \Sigma|F_o|$
$^b wR2 = [\Sigma[w(F_o^2-F_c^2)^2]/\Sigma[w(F_o^2)^2]]^{½}$
^{c}Quality-of-fit = $[\Sigma[w(F_o^2-F_c^2)^2]/(N_{obs}-N_{params})]^{½}$, based on all data.

Table S2. Selected bond distances (Å) and angles (º) for $[Cu(O_2C_{16}H_{23})]_\infty$ (**2**), $[Cu(O_2C_{16}H_{23})]_\infty$ (**3**), $[Cu_2(O_2C_{16}H_{23})_2] \cdot 2\ C_6H_4Cl_2$ (**4**), $[Cu(O_2C(3,5\text{-}CF_3)_2C_6H_3)]_\infty$ and $[Cu(O_2CC(CH_3)_3)]_\infty$.

	2	**3**	**4**	$[Cu(O_2C(3,5\text{-}CF_3)_2C_6H_3)]_\infty$	$[Cu(O_2CC(CH_3)_3)]_\infty$
Cu···Cu carb-bridged	2.9397(5)	2.8843(3)	2.4934(5)	2.693(2)-3.143(2)	2.850(2)-2.897(2)
Cu···Cu non-bridged	-		-	2.818(2)-3.008(2)	2.891(2)-3.125(2)
Cu–O carb^a	1.8445(3)	1.8483(12)	1.8729(12)	1.858(8)	1.850(7)
Cu–Cu–Cu	159.43(5)	96.224(11) 180.00	-	60.77(5)	62.64(5)

[a] Averaged.

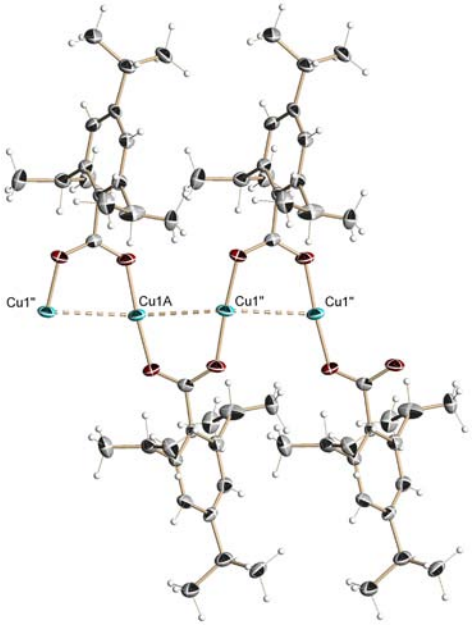

Fig. S1 An ORTEP drawing of the $[Cu(O_2C_{16}H_{23})]_\infty$ (**2**) fragment showing the Cu labeling scheme with thermal ellipsoids drawn at the 40% probability level. Only major parts of the two disordered isopropyl groups are shown. Cu blue, O red, C grey, H light grey. This color scheme is used in all figures.

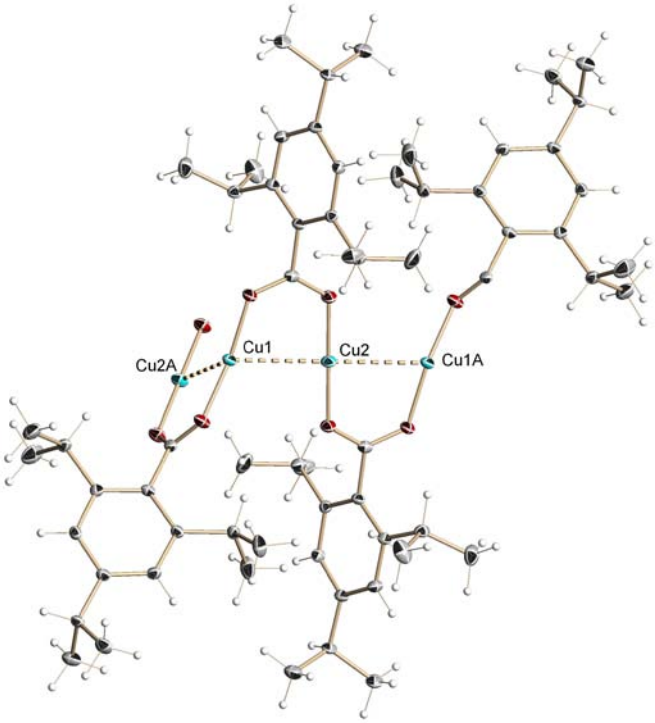

Fig. S2 An ORTEP drawing of the $[Cu(O_2C_{16}H_{23})]_\infty$ (**3**) complex.

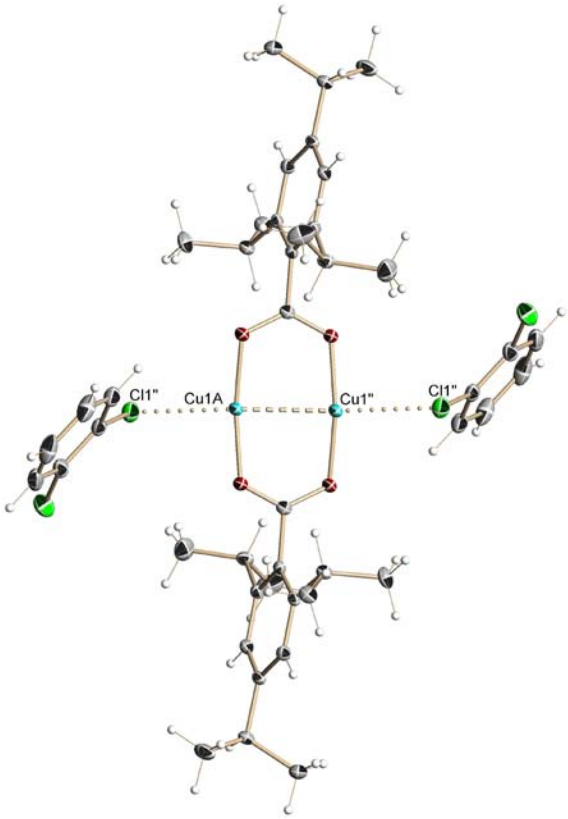

Fig. S3 An ORTEP drawing of the $[Cu_2(O_2C_{16}H_{23})_2]\cdot 2C_6H_4Cl_2$ (**4**) complex.

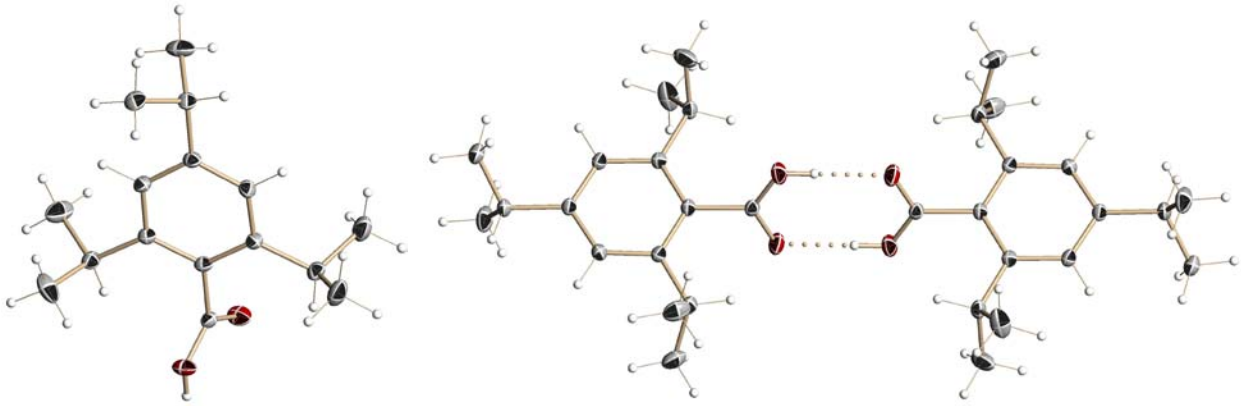

a b

Fig. S4 a) An ORTEP drawing of 2,4,6-triisopropylbenzoic acid. b) Formation of the dimers in the solid state via intermolecular hydrogen bonds.

X-ray powder diffraction details

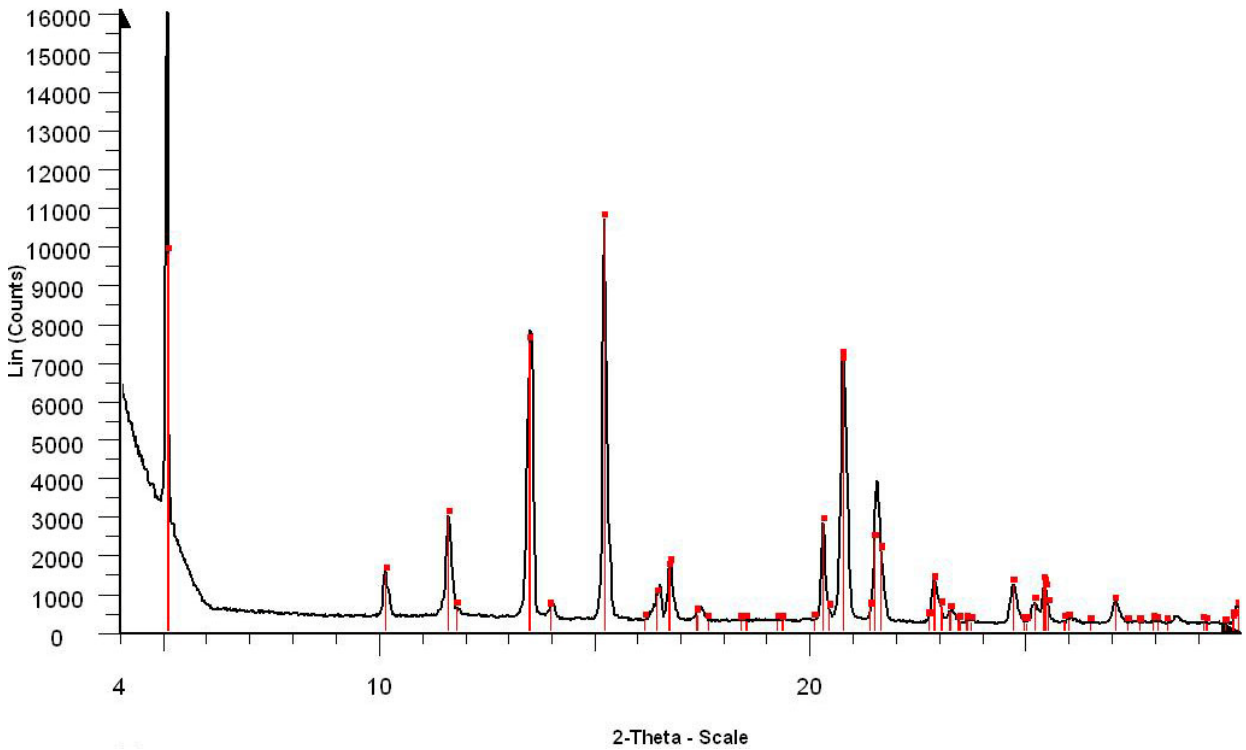

Fig. S5 The observed X-ray powder pattern for the bulk microcrystalline sample of **2** (black) *vs*. the simulated X-ray powder pattern based on the single crystal diffraction data of **2** (red).

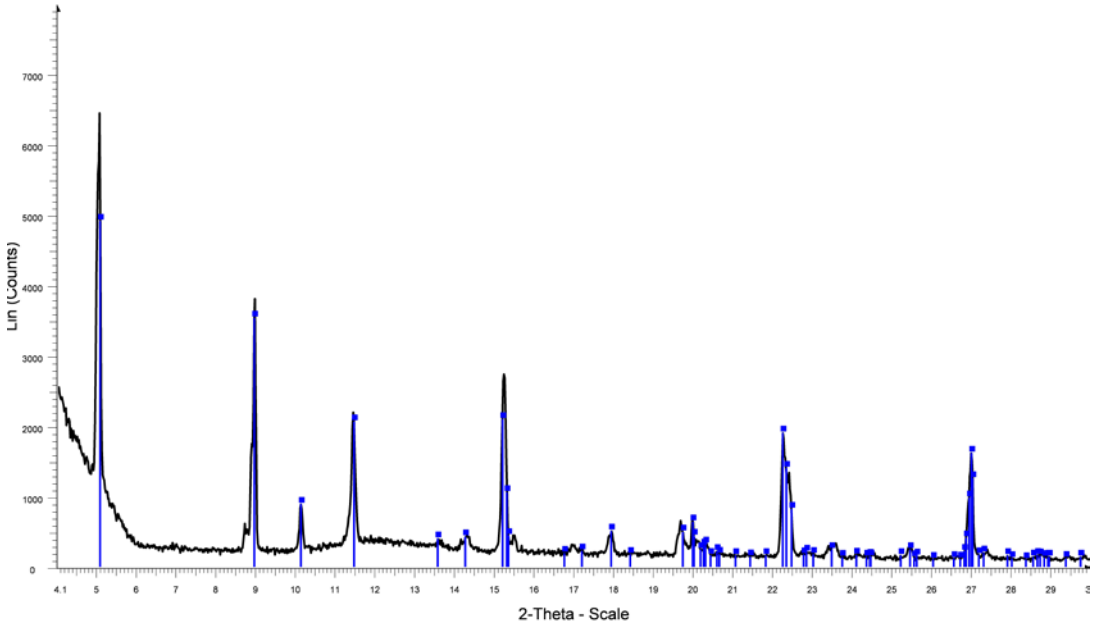

Fig. S6 The observed X-ray powder pattern for the bulk microcrystalline sample of **3** (black)

vs. the simulated X-ray powder pattern based on the single crystal diffraction data of **3** (blue).

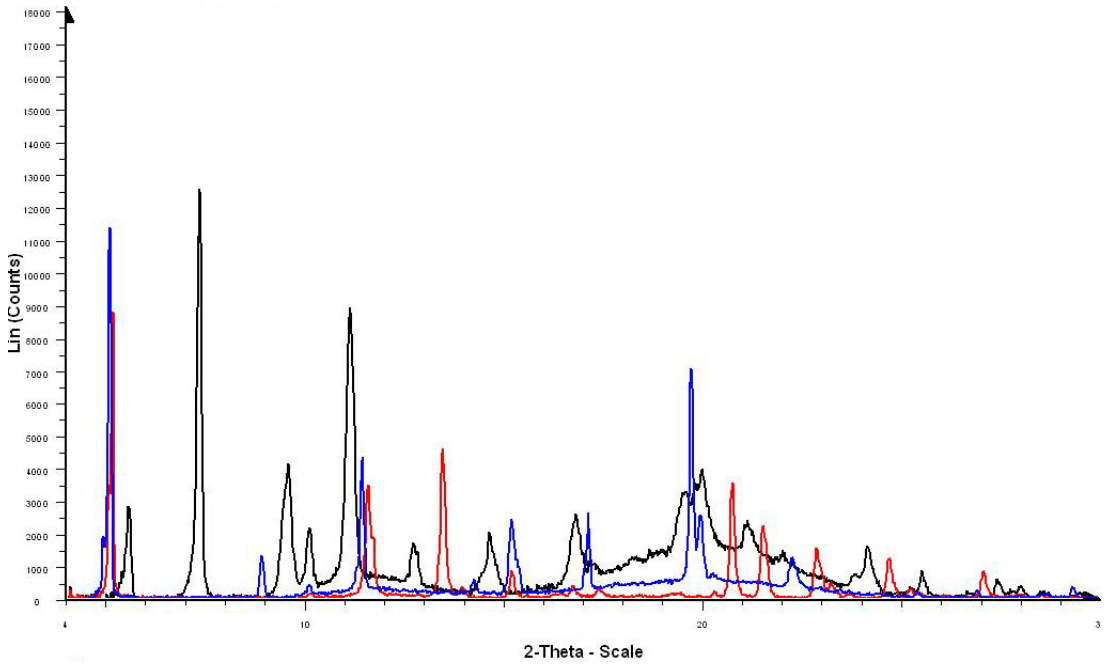

Fig. S7 The observed X-ray powder patterns for the bulk copper(I) 2,4,6-triisopropylbenzoate (black) *vs*. the bulk microcrystalline samples of **2** (red) and **3** (blue).

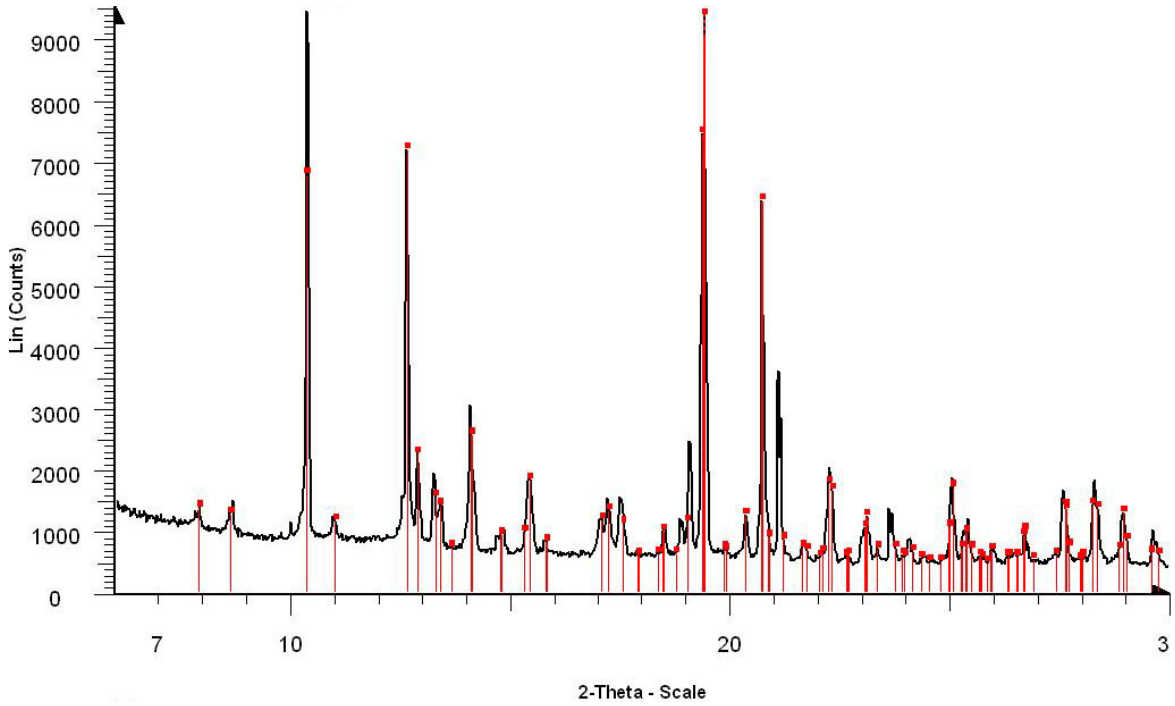

Fig. S8 The observed X-ray powder pattern for the single crystals of **4** (black) *vs*. the simulated X-ray powder pattern based on the single crystal diffraction data of **4** (red).

IR analysis

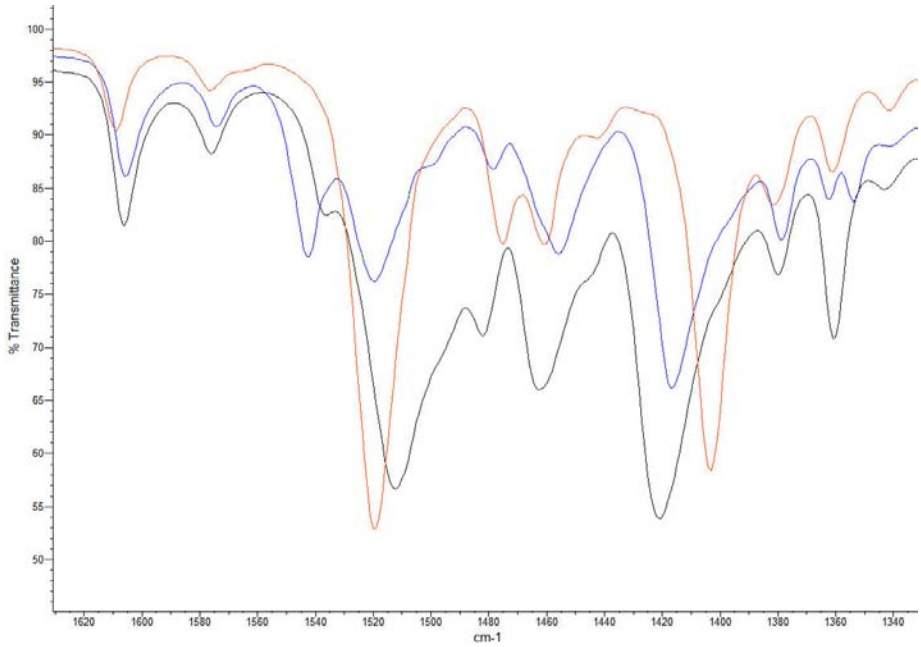

Fig. S9 IR spectra of **1** (red), **2** (black), and **3** (blue).

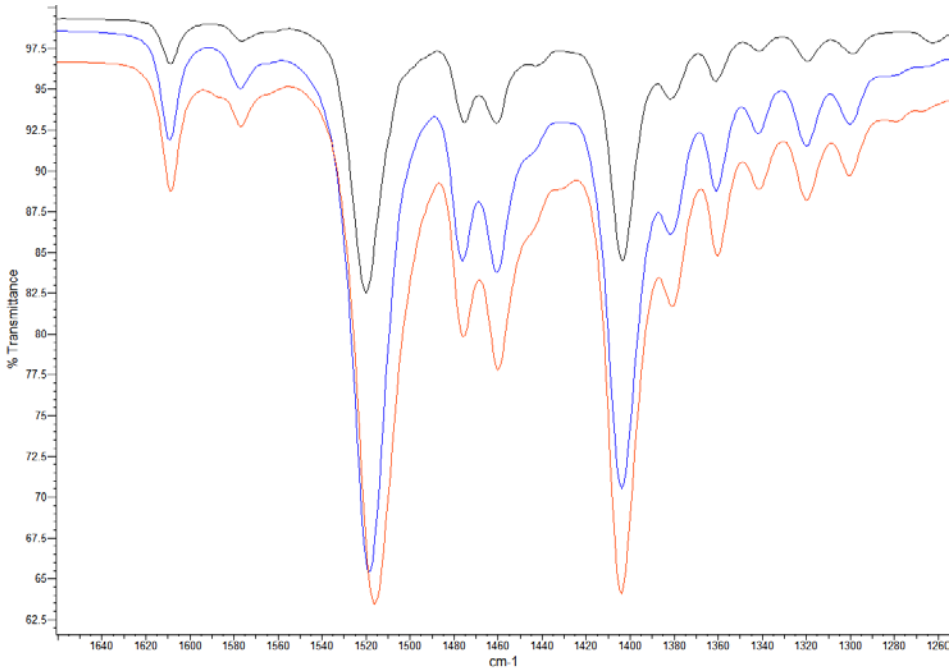

Fig. S10 IR spectra of **1** obtained by recrystallization from benzene/hexanes at room temperature (black), from hexanes at 95 °C (sealed ampoule, red), or from m-xylene 215 °C (sealed ampule, black).

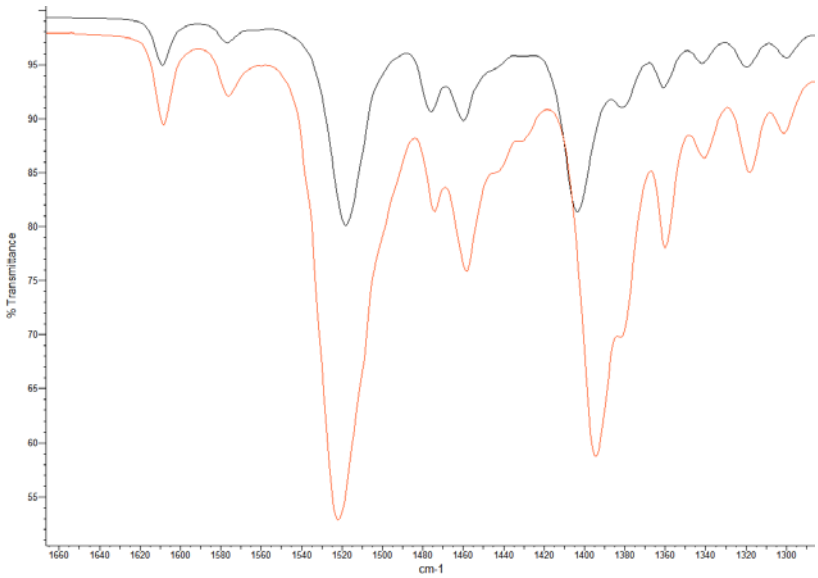

Fig. S11 IR spectra of **1** (black) and $[Ag_2(O_2C_{16}H_{23})_2]_\infty$ (red, see Fig. S12 for the corresponding $[Ag_2(O_2C_{16}H_{23})_2]_\infty$ structure).

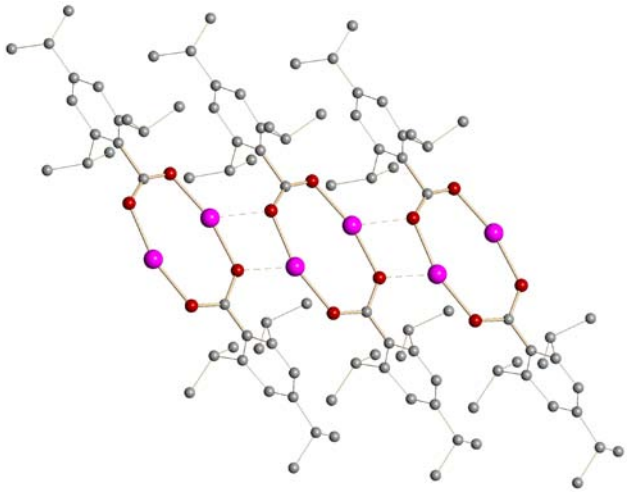

Fig. S12 A fragment of the $[Ag_2(O_2C_{16}H_{23})_2]_\infty$ polymeric chain. H atoms are omitted for clarity. The disordered solvent molecules filling voids in the crystal are not shown.

$[Ag_2(O_2C_{16}H_{23})_2]$ is not volatile (decomposes before reaching the sublimation temperature) and thus crystals cannot be grown from the gas-phase. Upon crystallization from solution (benzene, toluene, and m-xylene), aromatic solvents are co-crystallized with the $[Ag_2(O_2C_{16}H_{23})_2]_\infty$ chains

in the crystals. These facts preclude the direct comparison of the XRPD patterns simulated from single crystal data for silver(I) 2,4,6-triisopropylbenzoate and **1**.

TGA/DSC details

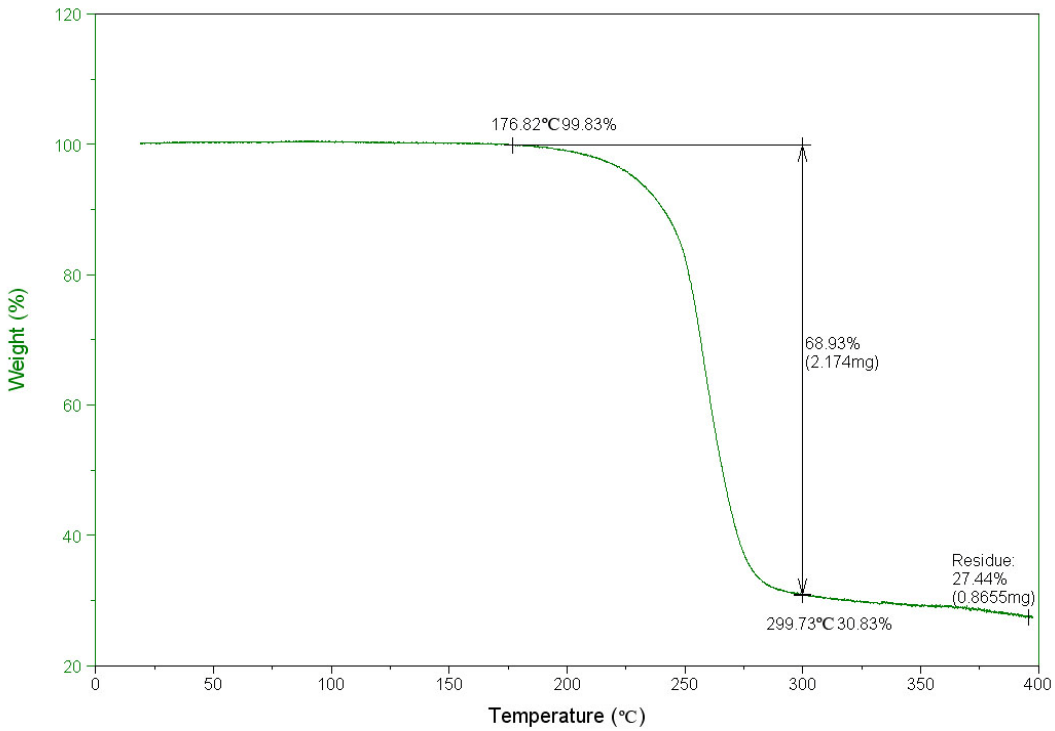

Fig. S13 TGA diagram of bulk [Cu($O_2C_{16}H_{23}$)] (**1**) (heating rate of 2°C/min).

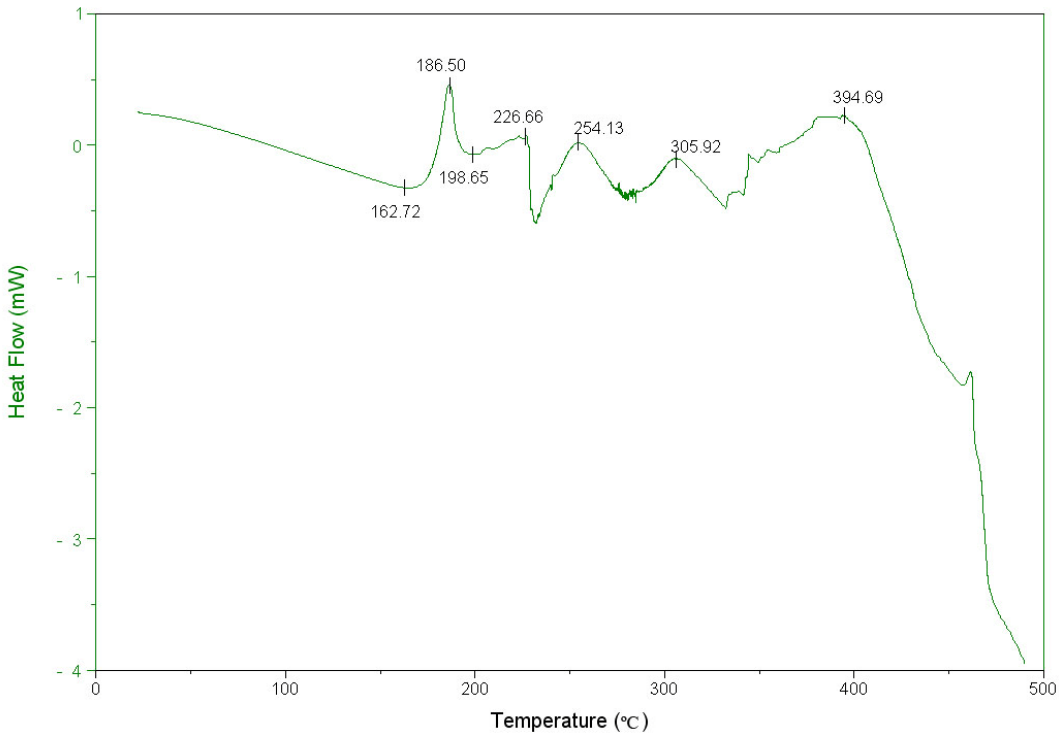

Fig. S14 DSC diagram of bulk $[Cu(O_2C_{16}H_{23})]$ (**1**) (heating rate of 2°C/min).

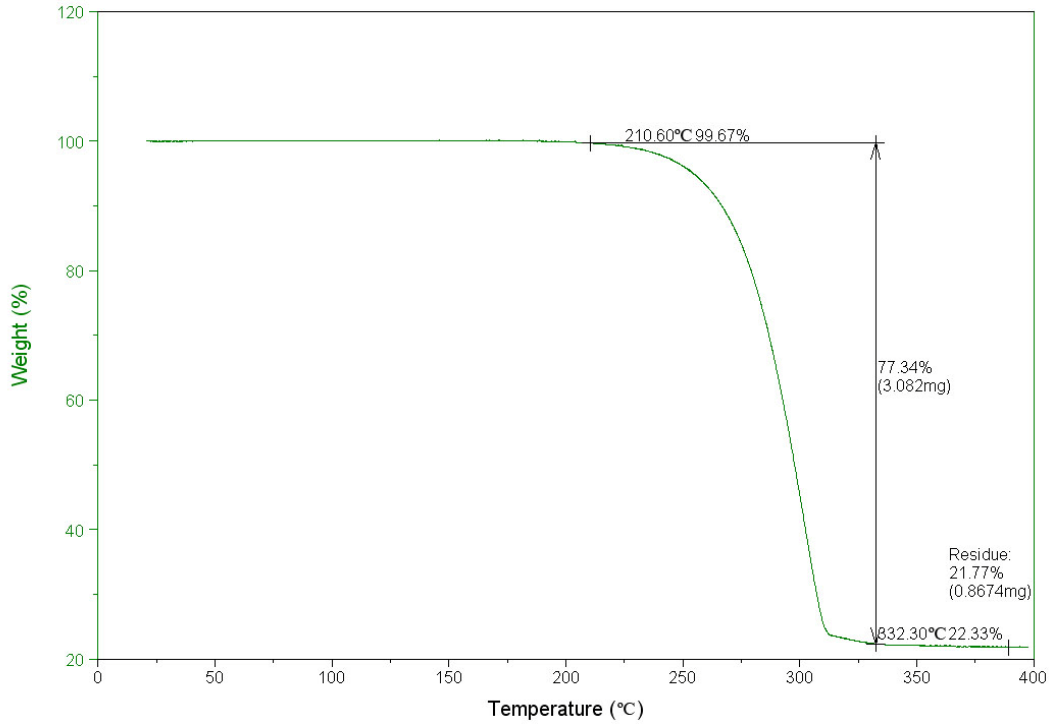

Fig. S15 TGA diagram of $[Cu(O_2C_{16}H_{23})]_\infty$ (**2**) (heating rate of 2°C/min).

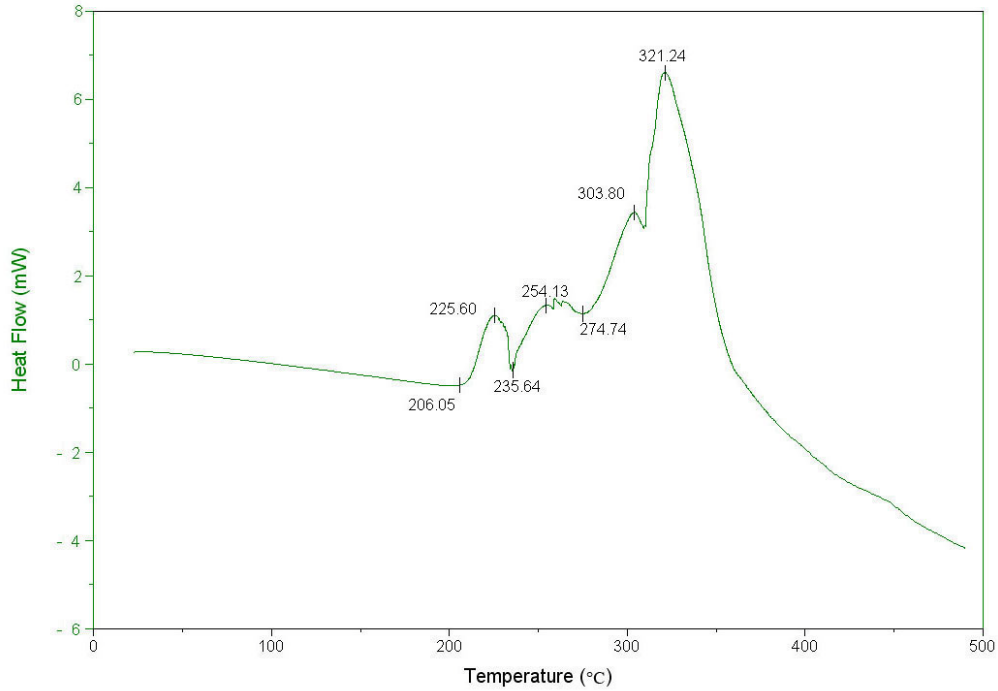

Fig. S16 DSC diagram of $[Cu(O_2C_{16}H_{23})]_\infty$ (**2**) (heating rate of 2°C/min).

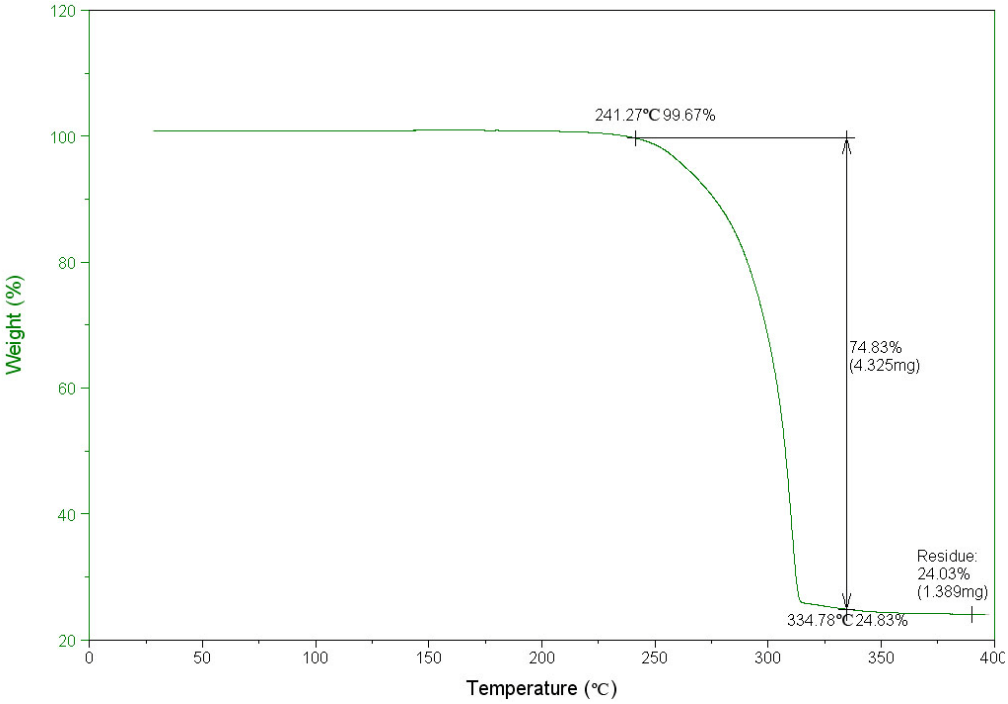

Fig. S17 TGA diagram of $[Cu(O_2C_{16}H_{23})]_\infty$ (**3**) (heating rate of 2°C/min).

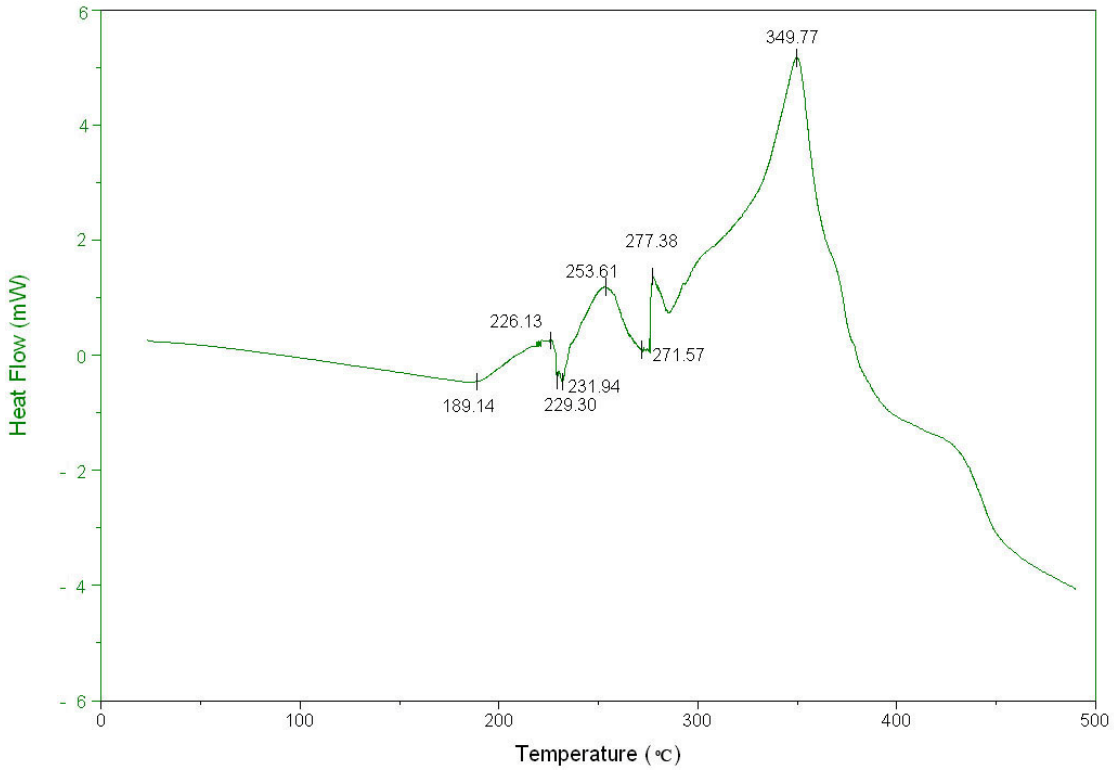

Fig. S18 DSC diagram of $[Cu(O_2C_{16}H_{23})]_\infty$ (**3**) (heating rate of 2°C/min).

References

[1] *SAINT*, version 6.02; Bruker AXS, Inc.: Madison, WI, 2001.

[2] *SADABS*; Bruker AXS, Inc.: Madison, WI, 2001.

[3] Sheldrick, G. M. *SHELX Acta Cryst.* 2008, **A64**, 112-122. *SHELXTL*, version 6.14; Bruker AXS, Inc.: Madison, WI, 2001.